Sun *et al. BMC Medical Genomics* (2025) 18:118
https://doi.org/10.1186/s12920-025-02187-4

BMC Medical Genomics

RESEARCH Open Access

A recurrent *ABCC2* c.2439 + 5G > A variant disturbs mRNA splicing and causes Dubin-Johnson syndrome

Rongyue Sun[1,3†], Ting Zhu[3†], Tingmin Zhou[3,4†], Yanzhao Luo[5], Tiantian Jiang[3], Chuangjie Gu[3], Ruiting Wu[3], Yue Wang[3], Fengzhen Xu[3], Shikang Fan[6], Dan wang[3*] and Yiming Chen[2*]

Abstract

Background Hyperbilirubinemia is the main clinical manifestation of Dubin-Johnson syndrome (DJS), of which most cases can be attributed to the variants in the *ABCC2* gene. This study aimed to characterize the mechanism of a splicing variant of the *ABCC2* gene and interrogate the variant pathogenicity.

Methods Whole exome sequencing (WES) was performed to identify potential genetic causes. Bioinformatics analysis was performed to predict the variant pathogenicity. Minigene assays were performed to investigate the effects of the identified variant on mRNA splicing. Western blot (WB) experiments were performed to verify the impact of the variant on protein expression. Protein subcellular localization was analyzed by indirect immunofluorescence (IF).

Results Genetic analysis revealed compound heterozygous variants in *ABCC2* gene: the splice-site variant c.2439 + 5G > A inherited from the mother and the nonsense variant c.3825 C > G (p.Y1275X) inherited from the father. The recurrent *ABCC2* c.2439 + 5G > A variant can affect mRNA splicing which leads to the skipping of exon 18 and induces the loss of 56 native amino acids, resulting in a shortened MRP2 protein (p.Gly758_Lys813del). The c.2439 + 5G > A variant may cause mislocalization of the mutant protein and significantly reduces its expression.

Conclusion Our study identifies c.2439 + 5G > A in *ABCC2* as a pathogenic variant underlying DJS through aberrant splicing. Critically, the proband's phenotype resulted from compound heterozygous variants leading to biallelic loss of functional protein. These findings highlight the necessity of comprehensive *ABCC2* genetic testing for DJS, facilitating accurate diagnosis and personalized patient management.

Keywords *ABCC2*, Dubin-johnson syndrome, Heterozygous intronic variant, Minigene assays

†Rongyue Sun, Ting Zhu and Tingmin Zhou contributed equally to this work.

*Correspondence:
Dan wang
wd608044@wmu.edu.cn
Yiming Chen
205146@wmu.edu.cn

Full list of author information is available at the end of the article

© The Author(s) 2025. **Open Access** This article is licensed under a Creative Commons Attribution-NonCommercial-NoDerivatives 4.0 International License, which permits any non-commercial use, sharing, distribution and reproduction in any medium or format, as long as you give appropriate credit to the original author(s) and the source, provide a link to the Creative Commons licence, and indicate if you modified the licensed material. You do not have permission under this licence to share adapted material derived from this article or parts of it. The images or other third party material in this article are included in the article's Creative Commons licence, unless indicated otherwise in a credit line to the material. If material is not included in the article's Creative Commons licence and your intended use is not permitted by statutory regulation or exceeds the permitted use, you will need to obtain permission directly from the copyright holder. To view a copy of this licence, visit http://creativecommons.org/licenses/by-nc-nd/4.0/.

Introduction

Bilirubin, a hemoglobin-derived pigment, is primarily generated during the catabolism of senescent or abnormal red blood cells—a crucial physiological process for maintaining erythrocyte homeostasis [1]. Hyperbilirubinemia serves as a significant clinical indicator, often signaling underlying hepatobiliary dysfunction across diverse etiologies [2]. Among the rare inherited disorders associated with conjugated hyperbilirubinemia, Dubin-Johnson syndrome (DJS) stands out as an autosomal recessive condition characterized by chronic or intermittent jaundice and hepatic deposition of dark pigmentation [3]. First described in 1954 [4], DJS was later linked to mutations in the *ABCC2* gene in 1997 [5]. Subsequent studies have identified a spectrum of pathogenic *ABCC2* variants, including missense, nonsense, splice-site, and deletion mutations—contributing to the molecular pathogenesis of this syndrome [6–10]. While patients typically present with jaundice and nonspecific abdominal discomfort, the clinical manifestations of DJS can vary in severity.

The *ABCC2* (NM_000392.5) gene, located on chromosome10q24, comprises 32 exons and encodes the 174 kDa multi-drug resistance protein 2 (MRP2). This ATP-dependent efflux transporter consists of 1,545 amino acids and is structurally characterized by 17 transmembrane helices, organized into three membrane-spanning domains (MSDs) and two nucleotide-binding domains (NBDs) [1]. As a member of the ATP-binding cassette (ABC) transporter superfamily, MRP2 is an integral membrane glycoprotein predominantly expressed at the apical membrane of hepatocytes [11]. It plays a critical role in the biliary excretion of endogenous and exogenous substrates, including conjugated bilirubin, glucuronide conjugates, xenobiotics, and various organic anions, through an energy-dependent transport mechanism [12].

The majority of the DJS-associated variants in *ABCC2* are related to the deficiency in MRP2 protein synthesis or secretion activities [13]. Some variants may affect the splicing function of mRNA. Pre-mRNA splicing is a critical step in eukaryotic gene expression, during which introns (non-coding intervening sequences) are precisely excised, and exons (including protein-coding sequences and untranslated regions, UTRs) are ligated to form mature mRNA [14]. Splicing mutations can cause the occurrence of various monogenic genetic diseases [15–17]. This suggests that splicing abnormalities caused by splicing variants are the pathogenesis of related monogenic genetic diseases.

In this work, we reported a DJS proband who presented with chronic conjugated hyperbilirubinemia persisting for 15 years. WES results indicated that the proband carried compound heterozygous variants in the *ABCC2* gene: the splice-site variant c.2439 + 5G > A (*ABCC2*: NM_000392.5: intron18) and the nonsense variant c.3825 C > G (*ABCC2*: NM_000392.5: exon27, p.Y1275X). These two variants had been previously reported [18, 19]. However, our work first investigated the potential mechanisms of variant c.2439 + 5G > A causes DJS, which affects the normal splicing of *ABCC2* mRNA and results in exon 18 skipping (r.2272_2439del). The aberrant splicing generated an in-frame deletion transcript (r.2272_2439del), which eliminates 56 amino acids (*p.Gly758_Lys813del*) within the nucleotide-binding domain 1 (NBD1) domain of MRP2 without introducing frameshifts or premature termination codons. Functional analysis revealed that the c.2439 + 5G > A variant significantly reduced MRP2 expression and impaired its organic anion transport activity. Furthermore, the mutant protein exhibited mislocalization, suggesting that this variant might lead to the loss function of MRP2 protein.

Materials and methods

Ethical compliance and consent to participate

The study was approved by the ethics committee of The First Affiliated Hospital of Wenzhou Medical University. Written informed consent was obtained before commencing the study.

Whole exome sequencing (WES) and sanger sequencing

Genomic DNA was extracted and purified from the proband and his families using TIANamp Genomic DNA Kit (Tiangen, Cat#DP304-03,Beijing, China), fragmented, and then captured using Agilent Sure Select Human All Exome V6 Kit (Agilent Technologies, Santa Clara, CA, USA).WES was performed by in-solution hybridization, followed by high-throughput paired-end sequencing on a NovaSeq 6000 platform (Illumina, Inc., San Diego, CA, USA) which has a sensitivity of > 99% to examine > 95% of the target regions, with a reading length of 150 bp. Burrows-Wheeler alignment tool (version 0.7.15) was used to align the sequence according to the hg38/GRCh38 human reference genome sequence. The variants were analyzed and annotated using the Verita Trekker Mutation Site Detection System and Enliven Variant Site Annotation Interpretation System (Berry Genomics, Shanghai, China). The databases include disease databases (HGMD, DECIPHER, ClinVar, UCSC, and OMIM) and population databases (gnomAD, 1000G, and dbSNP). According to the American College of Medical Genetics and Genomics guidelines (ACMG) [20], the pathogenicity of variants has five categories: pathogenic, likely pathogenic, uncertain significance, likely benign, and benign. Suspected variants were validated in the probands and their families using Sanger sequencing. Polymerase chain reaction (PCR) was performed to amplify exon and intron boundaries. The products were

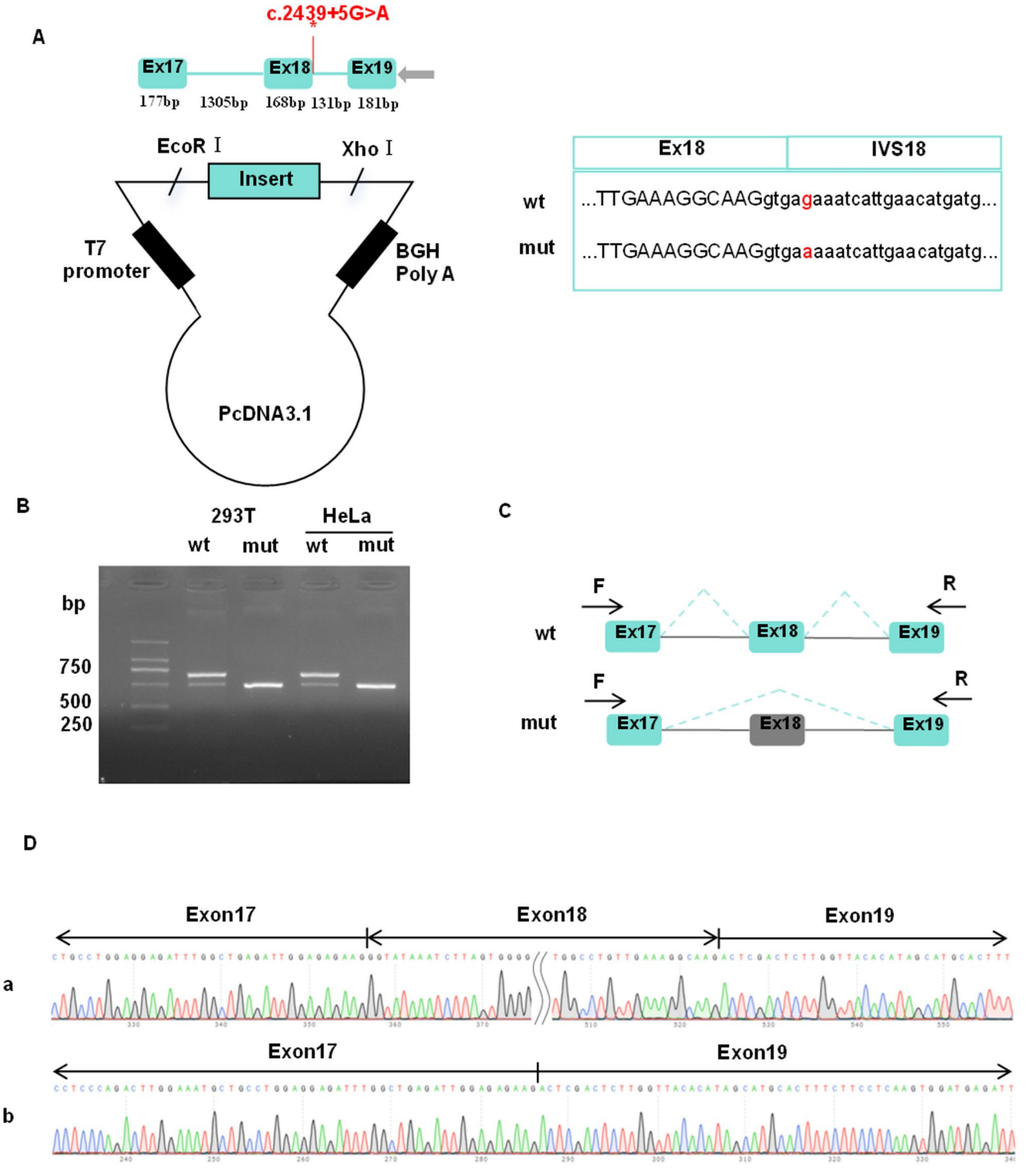

Fig. 1 Functional analysis of the *ABCC2* variant effect on mRNA splicing. (**A**) Construction strategy of pcDNA3.1 minigene vector, * representative of the variant site, the sequencing of wild-type *ABCC2* gene vector and c.2439 + 5G > A *ABCC2* variant gene vector. (**B**) Gel electrophoresis of reverse transcription polymerase chain reaction products displayed a single band a (estimated 670 bp) from the wild-type (wt) and a smaller band b (estimated 502 bp) in the mutant type (mut). (**C**) The splicing pattern corresponding to the band a and band b. (**D**) Illustration of the sequencing of band a (wild-type in HEK293T and Hela cells) and band b (variant c.2439 + 5G > A in HEK293T and Hela cells) products lead to a shorter transcript with deletion of exon 18 including 168 bp

sequenced using a 3500xL Genetic Analyzer (Applied Biosystems, Waltham, MA, USA).

In silico prediction assay

The splice mutation site was analyzed with SpliceAI (ht

Table 1 Primer sequences used to analyze the variant of the *ABCC2* gene and vector pcDNA3.1

Primer name	Primer sequence (5` – 3`)
34,034-ABCC2-F	CCACCACCCCATCTATGGAA
34,245-ABCC2-F	AACAAAAGTGGATGGGGCTT
36,736-ABCC2-R	GTTGTGCCACTGGTGTTTCT
36,959-ABCC2-R	TCTGAGACTACGCAACTGCC
ABCC2-mut-F	CCTGTTGAAAGGCAAGGTGAAAAATCATTGAACATGATGAA
ABCC2-mut-R	TTCATCATGTTCAATGATTTTTCACCTTGCCTTTCAACAGG
pcDNA3.1-ABCC2-EcoRI-F	GGTGGAATTCATGGGCACCACTGCCTATGTCCC
pcDNA3.1-ABCC2-XhoI-R	TAGACTCGAGGACTGTGGCTTCCTCTTCAGGG
pcDNA3.1-F	CTAGAGAACCCACTGCTTAC
pcDNA3.1-R	TAGACTCGAGGACTGTGGCTTCCTCTTCAGGG

tps://spliceailookup.broadinstitute.org/) and RDCC[SC] (https://rddc.tsinghua-gd.org/). The topological model of the human MRP2 transporter was generated using the online tool Protter (http://wlab.ethz.ch/protter/start/). The SWISS_MODEL (http://swissmodel.expasy.org/) was used to construct the three-dimensional structures of the protein variants.

Plasmids construction

Genomic DNA (gDNA) was used as the template to amplify the *ABCC2* target region spanning exons 17–19 along with flanking intronic sequences (introns 17 and 18) (Fig. 1A), ensuring retention of the native splicing regulatory elements. Nested PCR was performed to obtain the wild-type (wt) *ABCC2* gene fragment using two primer pairs: 34,034-*ABCC2*-F/36,959-*ABCC2*-R (outer primers) and 34,245-*ABCC2*-F/36,736-*ABCC2*-R (inner primers; see Table 1 for sequences). To generate constructs containing the heterozygous c.2439 + 5G > A variant, three additional primer pairs were designed: pcDNA3.1-*ABCC2*-EcoRI-F/pcDNA3.1-*ABCC2*-XhoI-R (for full-length amplification), pcDNA3.1-*ABCC2*-EcoRI-F/*ABCC2*-mut-R (for 5'-fragment with mutation), pcDNA3.1-*ABCC2*-XhoI-R/*ABCC2*-mut-F (for 3'-fragment with mutation). The PCR products were gel-purified and assembled into the pcDNA3.1 vector (Hitrobio Biotechnology Co., Ltd., Beijing, China) linearized by PCR, using a seamless cloning kit (Vazyme, Nanjing, China). The plasmids pcDNA3.1-*ABCC2*-wt (wild-type) and pcDNA3.1-*ABCC2*-mut (c.2439 + 5G > A) were validated

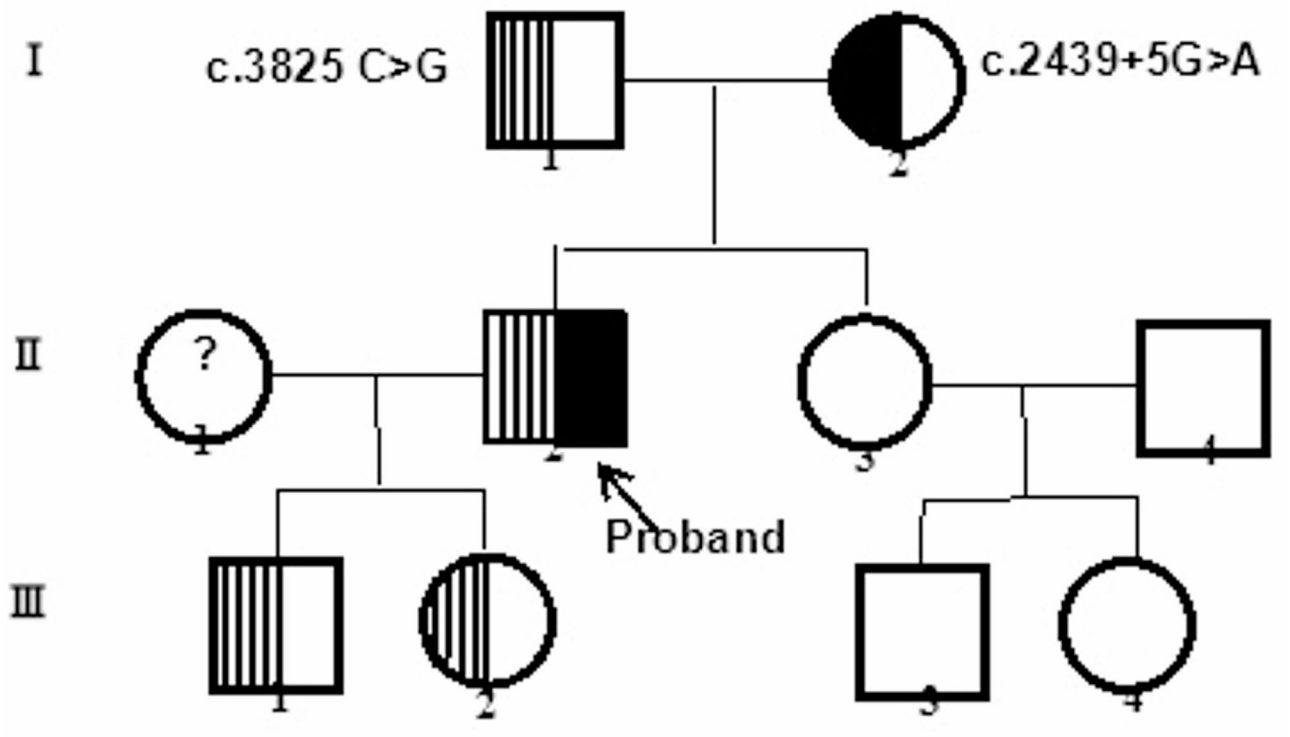

Fig. 2 Pedigree of the family. Circles and squares represent females and males, respectively. The black-filled symbols represent the proband

Table 2 Results of the prediction of the *ABCC2* c.2439 + 5G > A variant in spliceai

Variant	type	score
ABCC2: c.2439 + 5G > A	Acceptor Loss	0.46
	Donor Loss	0.63

by Sanger sequencing. To substantiate the conclusion drawn in this study, the assay was conducted repeatedly in another pcMINI-C vector using the same experimental method described above (Supplementary Figure). According to the results of the minigene experiment, we construct another plasmids: pCMV-FLAG-*ABCC2*-del (758-813aa)-Neo. The pCMV-EGFP-*ABCC2*-Puro plasmid expressing human *ABCC2* was purchased from Miaoling Bioscience (P39506, Wuhan, China). *ABCC2* wt cDNA was used as a template to generate an p.Gly758_Lys813del variant cDNA clone using I-5™ 2×High-Fidelity Master Mix (Tsingke, Beijing, China). Primer sequences for generating p.Gly758_Lys813del were as follows: F1: GCCACCATGGATTACAAGGATGACGACGATAAGatgctggagaagttctgca. F2: TTGGTACCGAGCTCGGATCCGCCACCATGGATTACAAG. F3: gattggagagaagactcgactcttggttacacat. R1: gtcttctctccaatctcagcca. R2: AACGGGCCCTCTAGACTCGAGCtagaattttgtgctgttcacattc. The underlined sequence represents the homologous arm, the red font represents the enzyme cleavage site, BamHI was the upstream enzyme cleavage site, and XhoI

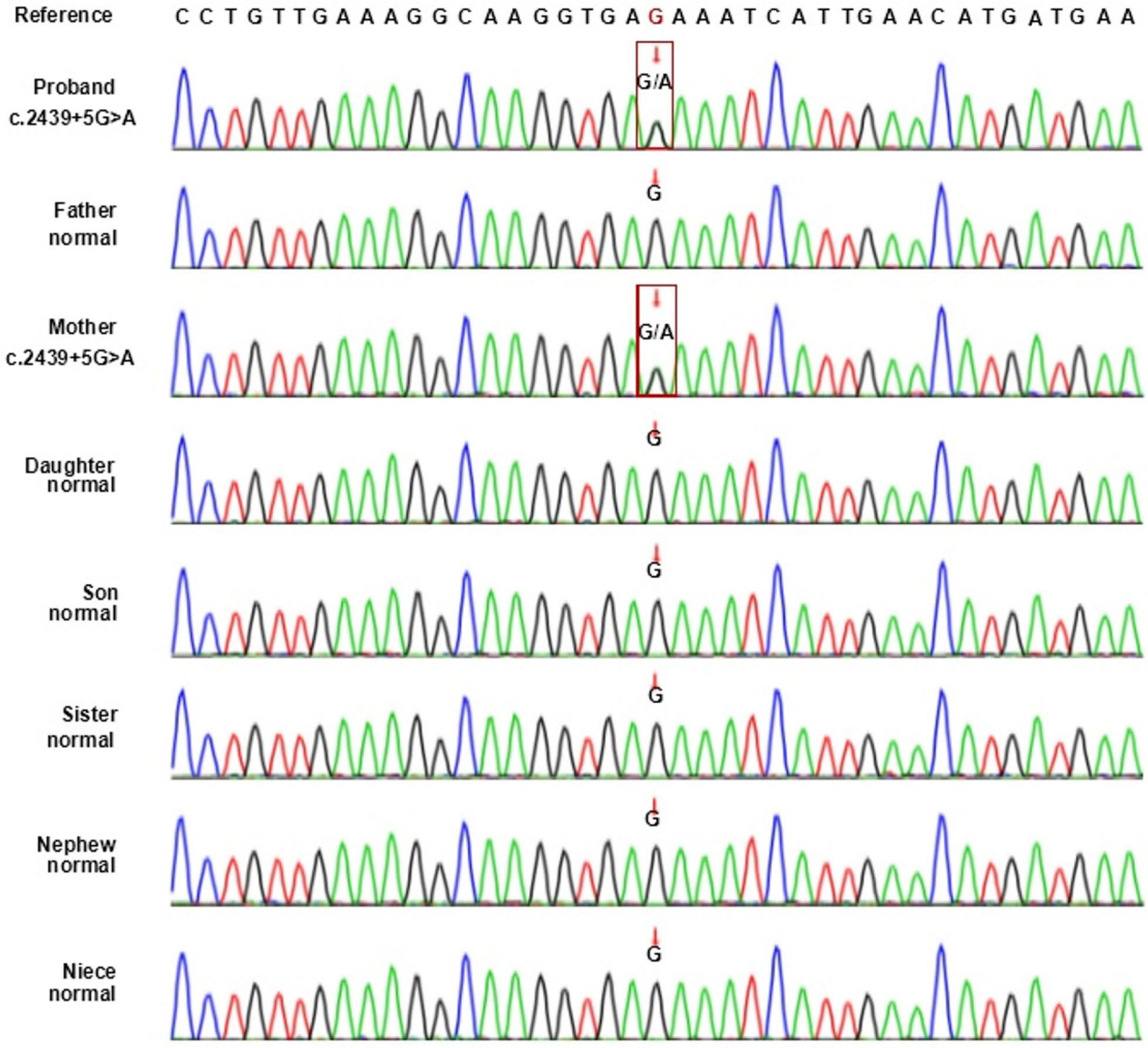

Fig. 3 The sequencing results of the family. The rectangular symbol indicates the variant site. The variant c.2439 + 5G > A is inherited from the mother

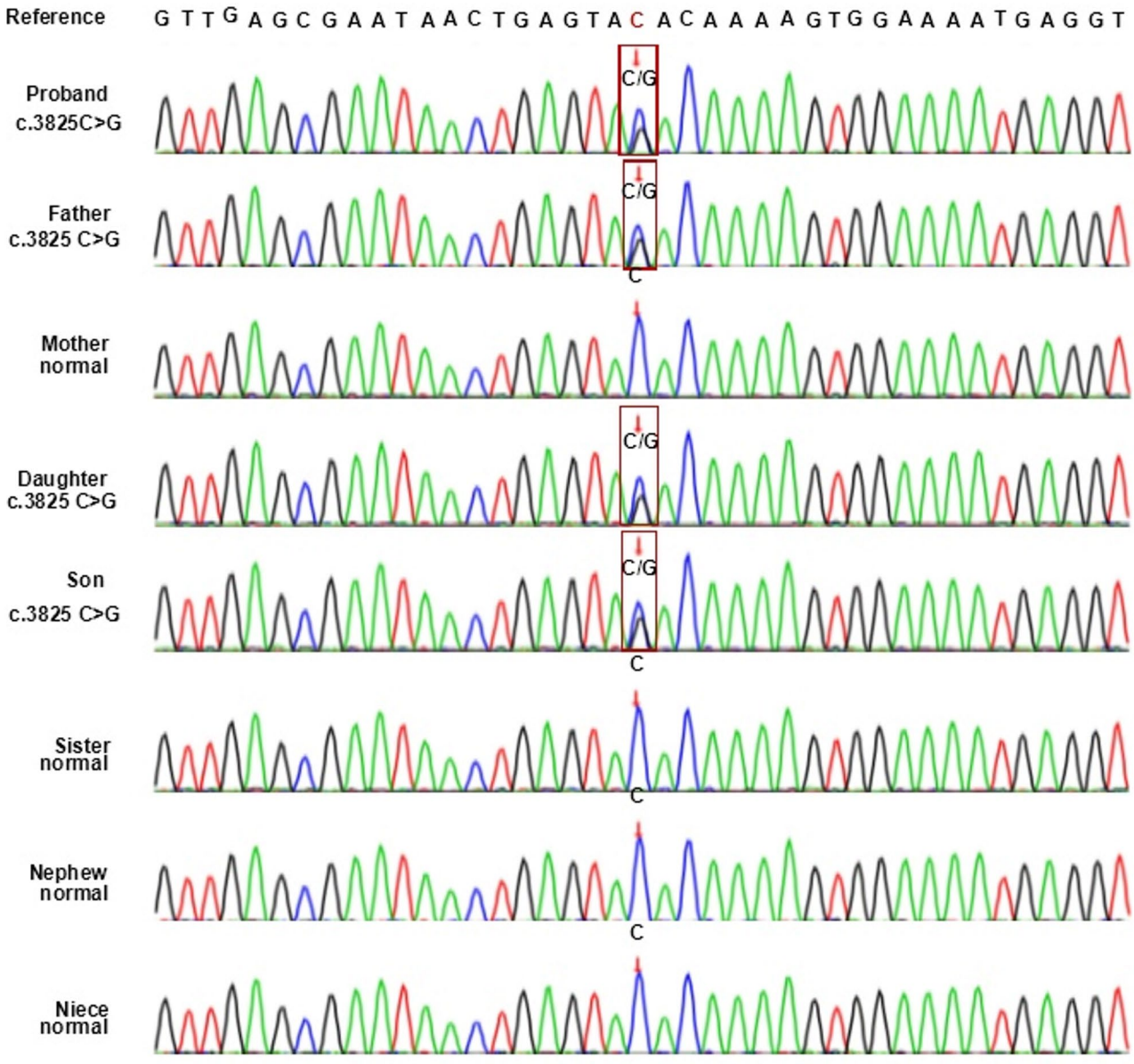

Fig. 4 The sequencing results of the family. The rectangular symbol indicates the variant site. The variant c.3825 C > G is inherited from the father

was the downstream enzyme cleavage site. All plasmids were confirmed by DNA sequencing.

Cell culture and transfection

To evaluate the functional impact of MRP2 variant, we selected the following cell models:

HuH-7 and HepG2: Human hepatoma cell lines with endogenous expression of hepatobiliary transporters, including MRP2, to mimic its physiological role in the liver, the primary site of DJS pathology. Human embryonic kidney (HEK293) and HeLa: Models with high transfection efficiency and negligible MRP2 background, enabling unambiguous assessment of mutant protein function. HEK293, human liver cancer cell lines (HuH-7 and HepG2) and HeLa cell lines (Cell Resource Center of the Chinese Academy of Medical Science, Beijing, China) were maintained at 37 °C with a humidified 5% CO_2 environment in Dulbecco's modified Eagle's medium (DMEM) supplemented with 10% fetal bovine serum and 1% penicillin-streptomycin. The cells were transfected when they reached 70% confluence in 6-well plates. According to the manufacturer's instructions of Lipofectamine 3000 (Thermo Fisher Scientific, Waltham, MA, USA), cells were transfected with equal amounts plasmids, each well was transfected with 2.5 μg of plasmid DNA. pcDNA3.1 was used as vector control. After labeling, the 6-well plate was returned to the incubator. After 24 h of culture, the medium in each well was aspirated

and replaced with fresh complete medium for further processing. The transfected cells were incubated for 48 h prior to further experimental procedures.

RNA extraction, PCR, and sequencing

FastPure Cell/Tissue Total RNA Isolation Kit V2 (Vazyme, Nanjing, China) was used to extract total RNA from transfected cells. DNA was degraded on a column with DNase I (Qiagen, Valencia, CA, USA). Extracted total RNAs were reverse-transcribed into cDNA, and reverse transcription polymerase chain reaction (RT-PCR) was performed using the primer pair pcDNA3.1-F/pcDNA3.1-R (Table 1). Then, the cDNA products were examined by 1% agarose gel electrophoresis and followed confirmed by Sanger sequencing. The length of wild-type cDNA products was determined to be 1987 bp in the pcDNA3.1-*ABCC2* vector and 861 bp in the pcMINI-C-*ABCC2* vector.

Western blot analysis

Cells were harvested using ice-cold PBS and lysed in RIPA buffer with protease inhibitors (Tris-HCl, 50 mM; Triton X-100, 1%; deoxycholate, 1%; NaCl, 150 mM; and SDS, 10%). Protein concentration was determined using the Pierce™ BCA Protein Assay Kit (ThermoFisher Scientific). The cell lysates were separated on 10% Tris-glycine sodium dodecyl sulfate-polyacrylamide gel electrophoresis gels and transferred onto PVDF membranes. Primary antibodies against MRP2 (1:1000; Abcam, Cambridge, MA, USA) and FLAG-tag (1:7500; Sigma-Aldrich, St. Louis, MO, USA) were used for western blot analysis according to standard protocols. After incubation with horseradish peroxidase (HRP)-conjugated secondary antibodies (1:8000) for 1 h at room temperature, Immobilon Western Chemiluminescent HRP Substrate (Thermo Fisher Scientific) was used to detect immunocomplexes on the membrane. Target protein band intensities were semi-quantified and normalized to GAPDH (1:2000, Cell signaling Technology, Danvers, MA, USA).

Indirect Immunofluorescence staining

Cells were fixed using 4% paraformaldehyde for 20 min and blocked with blocking buffer (BSA) for 1 h at room temperature. To detect MRP2 protein, cells were incubated with anti-MRP2 (1:300) as the primary antibody at 4 °C overnight. After washing with phosphate buffered saline (PBS) three times, cells were incubated with DyLight 594 goat anti-rabbit IgG antibody (1:500; Jackson ImmunoResearch, Baltimore, PA, USA) for 1.5 h at room temperature. Finally, the immunofluorescence of the cells was observed and photographed by a confocal microscope (TCS SP8; Leica, Wetzlar, Germany).

Measurement of organic anion transport activity

Organic anion transport activity was measured using monochlorobimane (MCB; Sigma-Aldrich C4528), a fluorescent MRP2 substrate (λ < sub > ex</sub>/λ < sub > em</sub> = 394/490 nm). Cells were pre-incubated with 0.2 mM MCB in ice-cold HBSS for 30 min to allow glutathione conjugation (GS-MCB formation) while inhibiting active transport. After washing, cells were incubated in pre-warmed HBSS (37℃) to initiate MRP2-mediated transport. Aliquots of extracellular medium were collected at 0, 5, 10, 30, 60, and 120 min. GS-MCB fluorescence was measured using a microplate reader (SpectraMax M5, Molecular Devices).

Statistical analysis

At least three different runs of each experiment were completed. Data are expressed as mean ± SD or Mean ± SEM, and the unpaired Student's *t*-test followed by Welch's correction was used to compare the two groups. The criterion for statistical significance was $P < 0.05$.

Results

Clinical data

The proband is a 35-year-old male who has a 15-year medical history of jaundice. Physical examination of liver function indicates total bilirubin (TB): 202 μmol/L, direct bilirubin (DB): 107 μmol/L, alpha-fetoprotein (AFP): 5.7 ng/mL, alanine transaminase (ALT): 35 U/L, and glutamic oxaloacetic transaminase (AST): 38 U/L. His mother has high levels of AFP, while his sister and nephew have hemophilia.

Variant detection

WES analysis identified the proband has the compound heterozygous variants of the *ABCC2* (NM_000392.5) gene: the splicing variant c.2439 + 5G > A, inherited from the mother (I-2, Fig. 2), the father, daughter, son, sister, nephew, and niece were wild-type (Fig. 3); the nonsense variant c.3825 C > G, inherited from the father (I-1, Fig. 2), his daughter and son have a heterozygous variant of c.3825 C > G in the *ABCC2* gene, while the mother, sister, nephew, and niece were wild-type (Fig. 4). Both variants were confirmed by Sanger sequencing and classified as pathogenic/likely pathogenic per ACMG guidelines (PVS1 + PM2 + PM3 for c.3825 C > G; PP1 + PM2 + PP3 + PM3 for c.2439 + 5G > A). No other pathogenic variants in *ABCC2* were detected.

In Silico assay

The Splice AI algorithm indicates that *ABCC2* c.2439 + 5G > A variant reduces the confidence score of the original acceptor site by 0.46 and the donor site by 0.63 (Table 2). The meaning of the value is the probability

of affecting splicing, the closer to 1 the greater the probability of affecting splicing. We also predicted the function of the *ABCC2* variant c.2439 + 5G > A using the RDDC^{SC} platform (https://rddc.tsinghua-gd.org/), two possible patterns of RNA splicing were predicted (Fig. 5A, B), indicated that the *ABCC2* intronic nucleotide substitution c.2439 + 5G > A is an mRNA splicing-affected variant. The predicted structure revealed a deletion of 56 amino acids (p.Gly758_Lys813del) within the nucleotide-binding domain 1 (NBD1) domain of MRP2 (Fig. 6A-D).

Minigene assay

To analyze the effect of the c.2439 + 5G > A variant on *ABCC2* mRNA splicing, minigne assay was conducted. The pcDNA3.1-*ABCC2*-wt minigene was 1962 bp and covered DNA regions including exon 17 (177 bp), intron 17 (1305 bp), exon 18 (168 bp), intron 18 (131 bp), and exon 19 (181 bp; Fig. 1A). A full-length 670 bp RT-PCR product of the expected normal size (partial plasmid sequence 144 bp and target gene 526 bp) was detected in HEK293T and HeLa cells transfected with pcDNA3.1-*ABCC2*-wt minigene as the most abundant transcript (Fig. 1B). Sanger sequencing confirmed that the 670 bp band corresponded to normal *ABCC2* mRNA, with exon 17-18-19 ligated and intervening intron 17–18 removed (Fig. 1C, D). The minigene construct containing the c.2439 + 5G > A variant in the pcDNA3.1-*ABCC2*-mut minigene was transfected into HeLa and HEK293T cell lines. In sharp contrast, normal *ABCC2* mRNA was not detected in the mutant (mut) lanes, except for one smaller band (502 bp; Fig. 1B). In the mut lanes, the shorter band of 502 bp corresponds to a misspliced transcript of *ABCC2* with complete skipping of exon 18; which only included exons 17 and 19 (Fig. 1C). The Sanger DNA chromatogram of the misspliced transcript of *ABCC2* is shown in Fig. 1D. We also used the pcMINI-C vector to confirm these results, which contains the general MCS-Intron B-Exon B by the same experimental procedure. Full-length sequence translation analysis of misspliced transcripts identified by minigene analyses indicated that this variant induces complete skipping of exon 18 including 168 bp nucleotides (c.2272_2439del), resulting in the loss of 56aa inside the shorter protein (p.Gly758_Lys813del). These results were consistent with the prediction of in silico assays, and the pattern of RNA

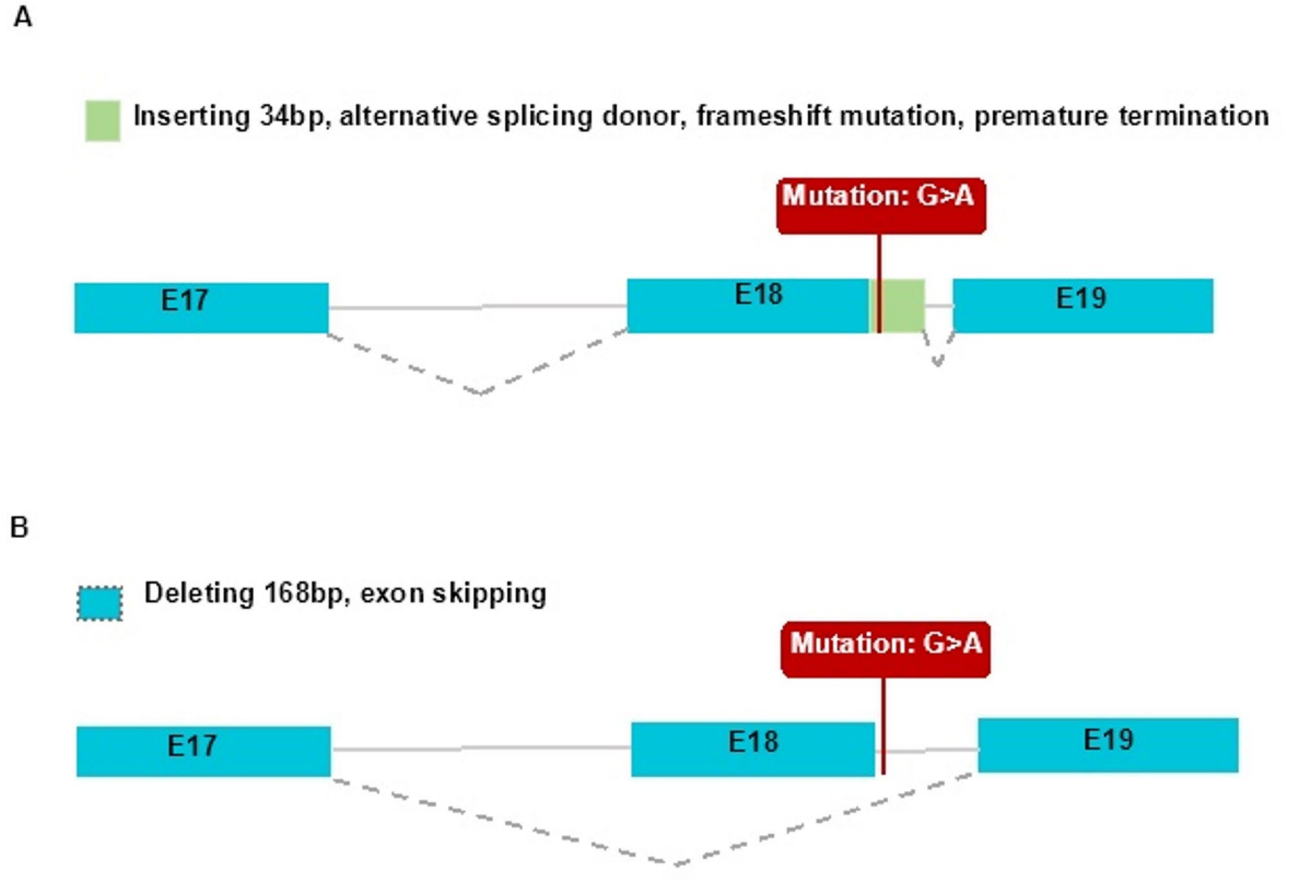

Fig. 5 Two patterns of RNA splicing prediction. (**A**). Pattern one: Inserting 34 bp, alternative splicing donor, frameshift mutation, premature termination. (**B**). Pattern two: Deleting 168 bp, exon skipping. E17: exon 17; E18: exon 18; E19: exon 19

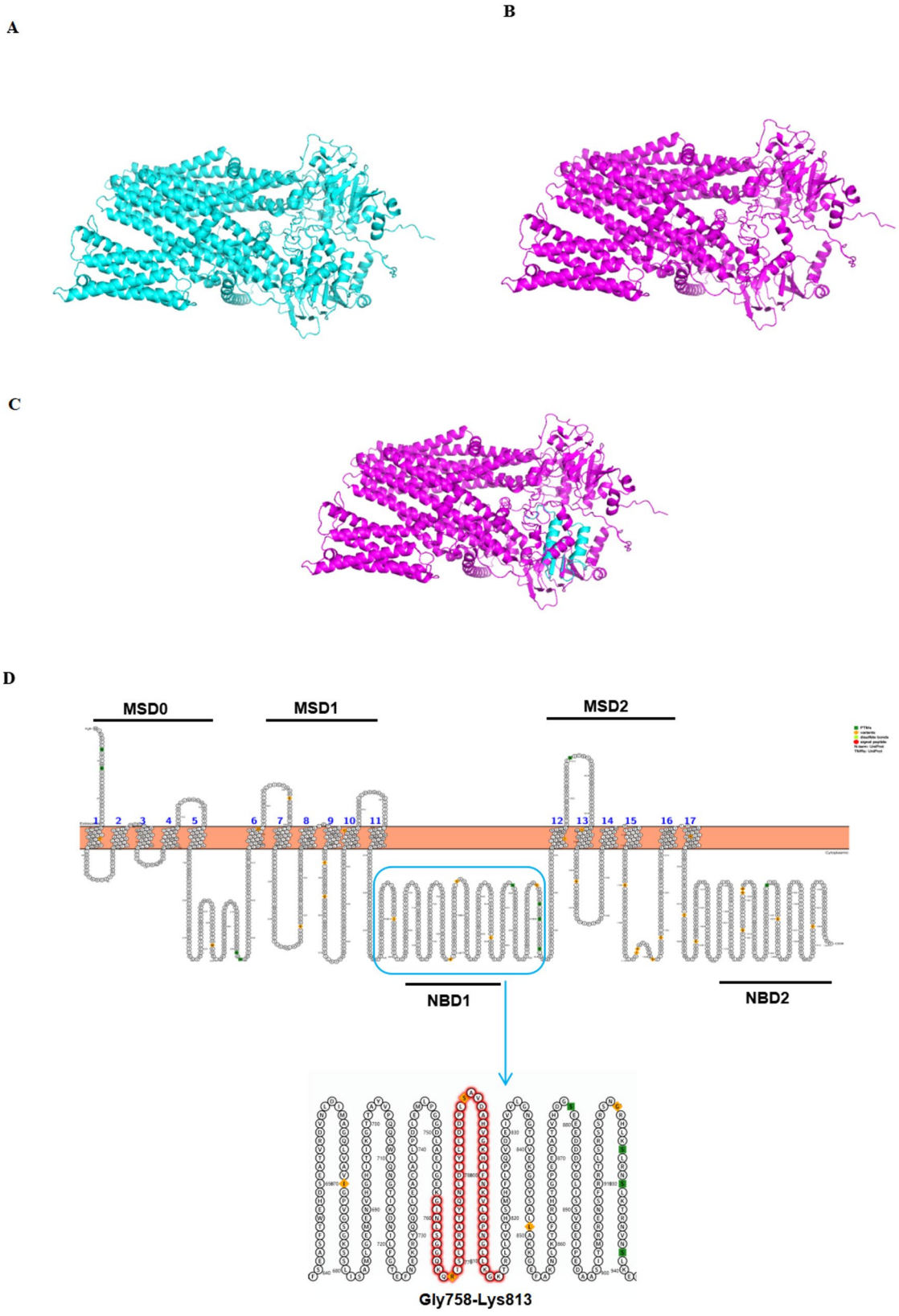

Fig. 6 Prediction of MRP2 structure and domain. (**A**) Wild-type MRP2 protein. (**B**) Mutant MRP2 (p.Gly758_Lys813del). (**C**) Compared wild-type and mutant MRP2 protein. RMSD: 32.8021 Å. (**D**) Predicted MRP2 protein domains showed the loss of 56aa (p.Gly758_Lys813del) located in nucleotide-binding domain 1 (NBD1) domain

splicing was validated to be consistent with the prediction of splicing pattern two (Fig. 5B).

MRP2 expression was decreased in cell lines expressing MRP2 c.2439 + 5G > A

ABCC2 gene encodes MRP2 protein. To investigate the effect of c.2439 + 5G > A, an equal amount of plasmid expressing wild type (WT) and mutant *ABCC2* were transfected into cell lines. To ensure accurate transiently expressed *ABCC2*, the *ABCC2* gene was placed just in front of three repeated FLAG tags. Western blotting found that the protein levels of MRP2 c.2439 + 5G > A protein were only 57 ± 2.39% and 50 ± 2.39% (both $p < 0.0001$, $n = 3$) that of wild-type MRP2^{WT} in HuH-7 and HepG2 cell lines, respectively (Fig. 7A, B, D, E). The co-expressed Flag tag showed that the protein levels were only 59 ± 2.39% and 55 ± 2.39% (both $p < 0.001$, $n = 3$) within these groups, respectively (Fig. 7C, F).

The *ABCC2* c.2439 + 5G > A variant May affect subcellular localization

To investigate whether the *ABCC2* c.2439 + 5G > A leads to subcellular mislocalization, we transfected HEK293T cells with FLAG-tagged *ABCC2* constructs and detected the MRP2 protein by immunofluorescence analysis. The results of fluorescence showed that MRP2^{WT} localized to the cell membrane and cytoplasm, while the MRP2 c.2439 + 5G > A mutant was significantly reduced both in the cell membrane and cytoplasm (Fig. 8A, B). These findings suggest that this variant might potentially alter the subcellular localization of MRP2 protein.

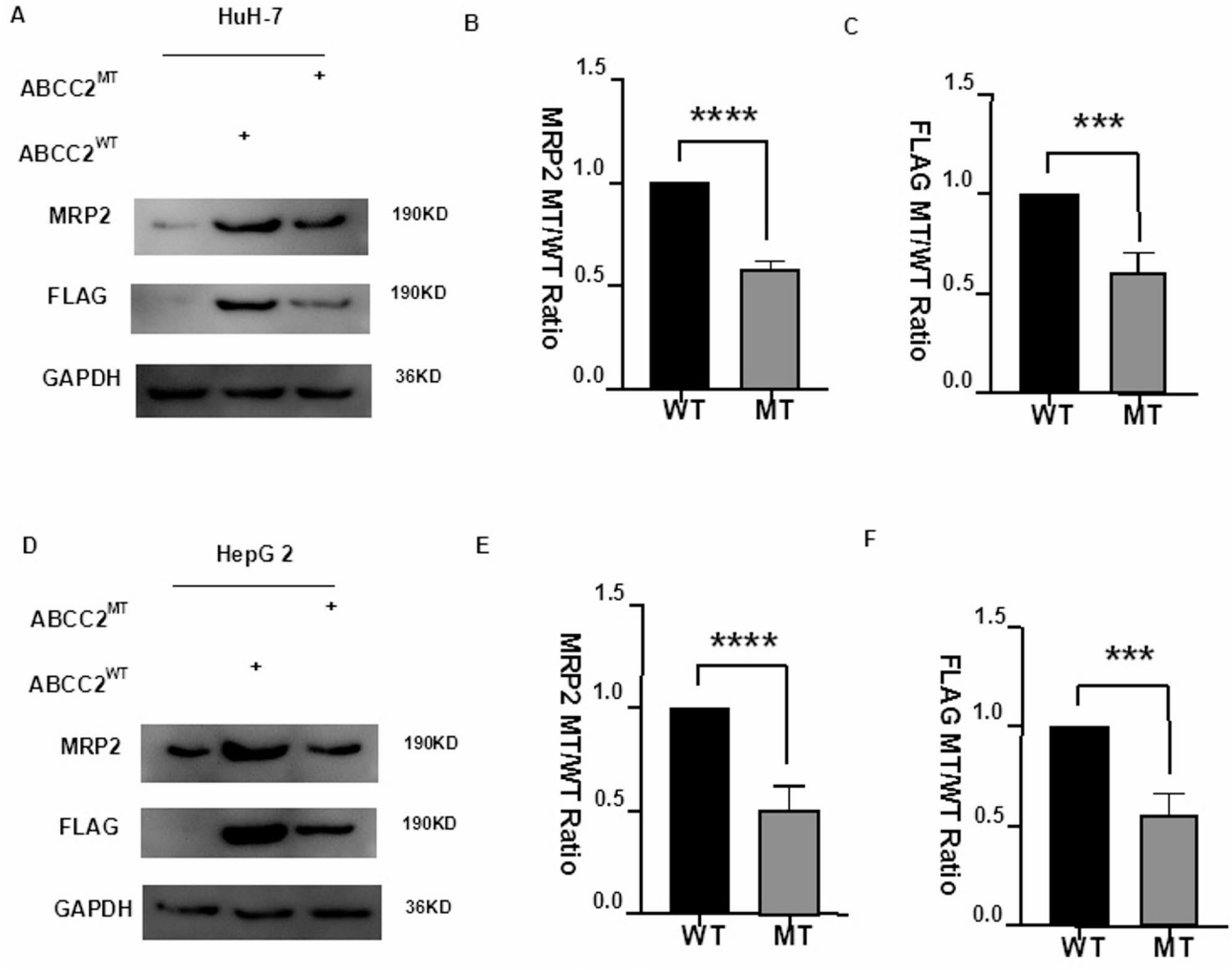

Fig. 7 The protein expression of MRP2 p.Gly758_Lys813del was decreased in cell lines. (**A**, **D**) Western blot bands demonstrated that the protein levels of over-expressed MRP2^{MT} were significantly lower than that of MRP2^{WT}. (**B**, **E**) The quantification found that the protein levels of MRP2^{MT} were only 57 ± 2.39% and 50 ± 2.39% (both $p < 0.0001$, $n = 3$) that of wild-type MRP2^{WT} in HuH-7 and HepG2 cell lines, respectively. (**C**, **F**) The co-expressed Flag tag showed that the protein levels were only 59 ± 2.39% and 55 ± 2.39% (both $p < 0.001$, $n = 3$) within these groups, respectively. All data are expressed as Mean ± SEM. Asterisks (*) represent statistically significant differences (***$P < 0.001$, ****$P < 0.0001$, $n = 3$). WT: wild-type MRP2; MT: MRP2 p.Gly758_Lys813del

Organic anion transport activity assay

To functionally validate the impact of *ABCC2* c.2439 + 5G > A on MRP2-mediated transport, we quantified the efflux of monochlorobimane (MCB) in transfected cells. MCB is selectively conjugated to glutathione (GSH) intracellularly, forming GS-MCB, which is exported by MRP2. This assay directly reflects MRP2's ability to transport conjugated anions. GS-MCB in the medium of Huh-7 and HepG-2 cell lines expressing wild-type MRP2 were significantly higher compared to those in cells expressing variant MRP2 (*ABCC2* c.2439 + 5G > A) ($p < 0.001$) (Fig. 9). The results indicated that the variant MRP2 (*ABCC2* c.2439 + 5G > A) has significantly reduced organic anion transport activity compared to the wild-type MRP2 ($P < 0.001$).

Discussion

In our study, we identified compound heterozygous variants in the *ABCC2* gene (c.2439 + 5G > A and c.3825 C > G) in a proband with DJS, characterized by chronic conjugated hyperbilirubinemia persisting for 15 years. While the proband exhibited typical DJS manifestations—elevated total bilirubin (TB: 202 μmol/L) and direct bilirubin (DB: 107 μmol/L)—the absence of severe liver dysfunction (normal ALT/AST) aligns with the benign clinical course often observed in DJS. However, the molecular mechanisms underlying these phenotypic features warrant deeper exploration to bridge the gap between genetic findings and clinical presentation.

The heterozygous intronic variant c.2439 + 5G > A was inherited from the mother, which has been previously reported [19], but its underlying mechanism has not been studied. In silico and in vitro minigene splicing assay indicated that c.2439 + 5G > A was a spliceogenic variant resulting in complete skipping of exon 18 (c.2272_2439del) in *ABCC2* gene. The aberrant splicing resulted in an in-frame deletion of 56 amino acids (p.Gly758_Lys813del) in the MRP2 protein, without introducing a downstream frameshift or a premature termination codon in the mRNA transcript. Functional analyses revealed that the mutant MRP2 protein exhibited significantly reduced expression levels and impaired organic anion transport activity compared to the wild-type protein, indicating that this variant might lead to loss function of MRP2 protein. According to the gnomAD database, this variant demonstrates an extremely low allele frequency (0.000007969) in the general population, effectively excluding the possibility of it being a benign polymorphism.

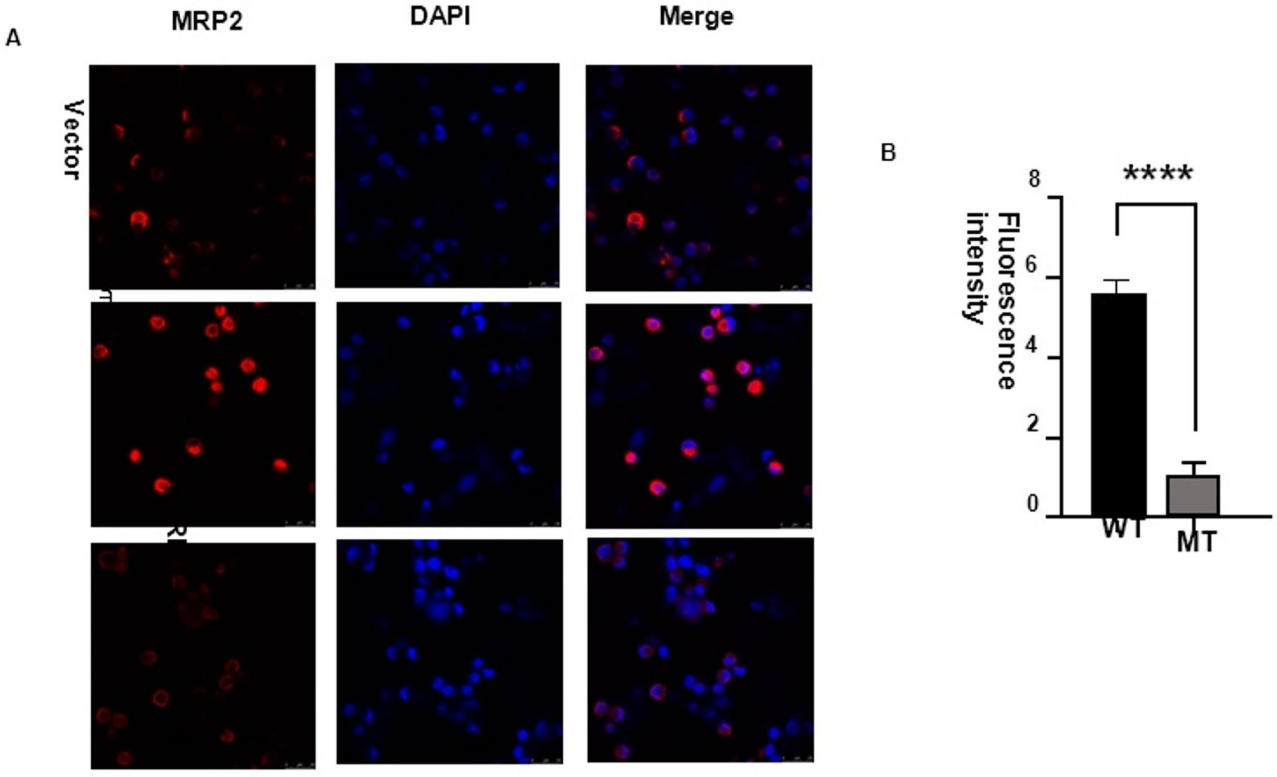

Fig. 8 The subcellular localization of MRP2 p.Gly758_Lys813del. (**A**, **B**) Immunofluorescence assay showed the decreased MRP2 p.Gly758_Lys813del expression both in cell membrane and cytoplasm. All data are expressed as Mean ± SEM. Asterisks (*) represent statistically significant differences (****$P < 0.0001$, $n = 3$). WT: wild-type MRP2; MT: MRP2 p.Gly758_Lys813del

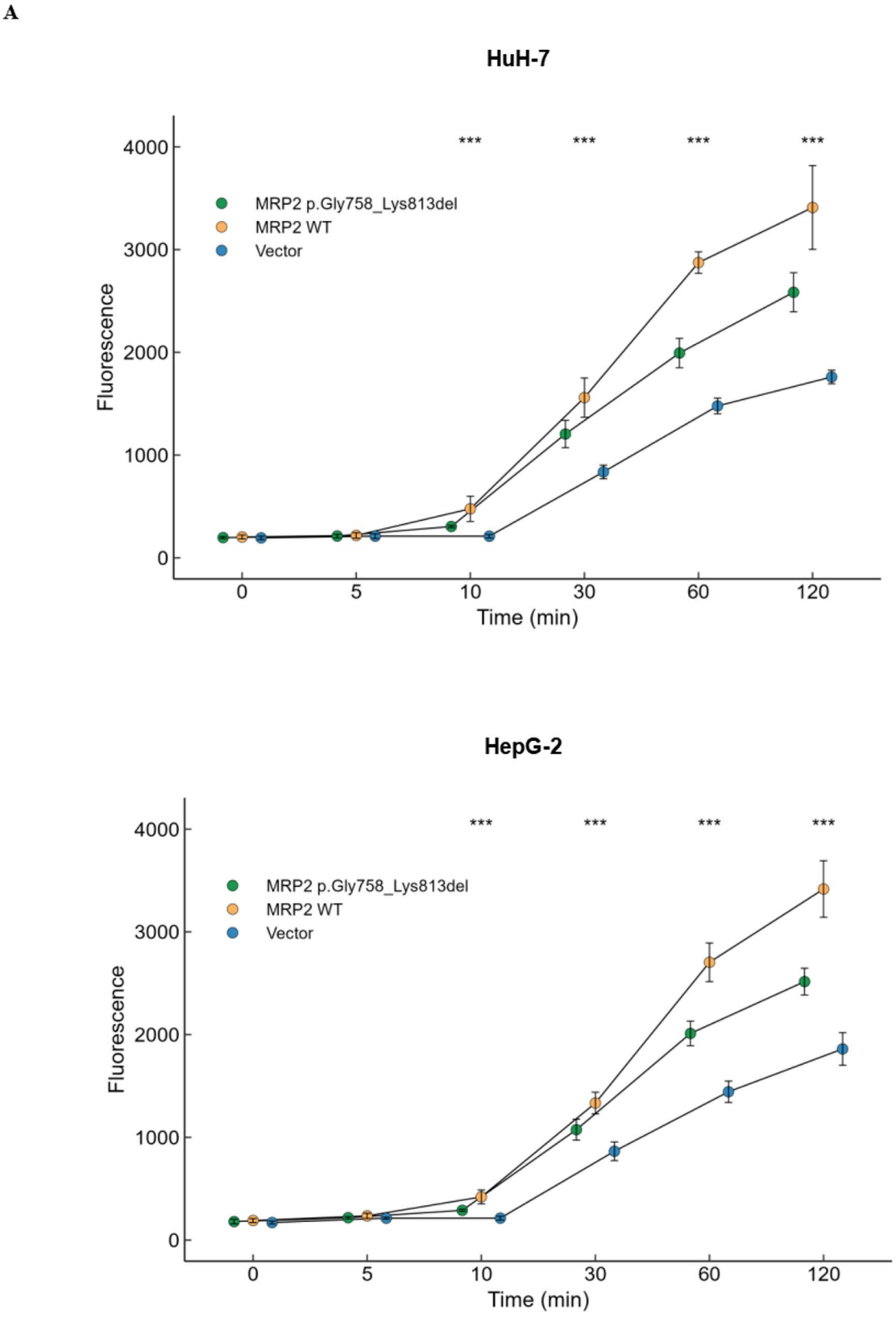

Fig. 9 MRP2 p.Gly758_Lys813del mutant exhibited decreased organic anion transport activity. Compared to wild-type MRP2, the MRP2 p.Gly758_Lys-813del mutant exhibited decreased organic anion transport activity in Huh-7 and HepG2 cell lines. (*) represent statistically significant differences (***$P < 0.001$, $n = 5$). Each bar represents the Mean ± SD

DJS is an autosomal recessive genetic disorder characterized by conjugated hyperbilirubinemia in liver function tests and *ABCC2* gene mutations [21]. The *ABCC2* gene encodes the MRP2 protein, which is mainly distributed in the bile duct membrane of hepatocytes [22]. It actively transports substrates to the extracellular by hydrolyzing ATP and is the main carrier protein for the excretion of various organic anions [23, 24]. Also, MRP2 was reported as an anion pump protein and highly expressed in various tumors, it causes the efflux of chemotherapy agents, leading to tumor drug resistance [24, 25]. DJS patients present with long-term or intermittent jaundice, elevated levels of conjugated bilirubin in serum, pathological manifestations of lysosomal melanin deposition in liver tissue, elevated levels of urinary fecal porphyrin type I, and significantly reduced expression of MRP2 protein [3, 26]. However, most patients have a good prognosis. For patients with high bilirubin levels and recurrent episodes, phenobarbital treatment can be considered, it was first reported in Japan in 1991 [27]. The combination of phenobarbital and ursodeoxycholic acid is safe and effective in the treatment of DJS patients, especially in patients with onset in the neonatal period [3, 18, 28]. The function of phenobarbital is to enhance the uptake and binding of bilirubin by increasing the activity of bilirubin glucuronosyltransferase [27, 28], and to stimulate the formation of hydroxylated bile acids through microsomal cytochrome P450-dependent enzymes [29], which are then excreted from urine. The molecular mechanism of the action of ursodeoxycholic acid includes stimulating the output pumps of MRP2, BSEP, and MRP3, MRP4 at the transcriptional and post-transcriptional levels, which then reduce the levels of serum conjugated bilirubin [30].

The c.2439 + 5G > A variant disrupts mRNA splicing, leading to exon 18 skipping (r.2272_2439del) and an in-frame deletion of 56 amino acids (p.Gly758_Lys813del) in the NBD1 domain of MRP2. This domain is critical for ATP hydrolysis, which powers MRP2-mediated transport of conjugated bilirubin and other organic anions. The loss of NBD1 functionality likely explains the proband's hyperbilirubinemia, as impaired ATP binding would reduce biliary excretion of bilirubin-glucuronides. Notably, the proband's bilirubin levels were comparable to those reported in other NBD1-domain mutations [31, 32], supporting the variant's pathogenicity and the genotype-phenotype consistency in DJS. The nonsense variant c.3825 C > G (p.Y1275X) further exacerbates MRP2 deficiency by introducing a premature termination codon, truncating the protein and likely triggering nonsense-mediated decay [18, 33, 34]. This compound heterozygous state results in near-complete loss of functional MRP2, consistent with the proband's marked hyperbilirubinemia. Importantly, the proband's parents—each carrying only one variant—were asymptomatic, underscoring the autosomal recessive nature of DJS and the threshold effect of MRP2 activity.

While this study provides mechanistic insights into the functional impact of *ABCC2* c.2439 + 5G > A, several limitations should be acknowledged. The analysis was restricted by the limited availability of biological samples from the proband, precluding transcriptomic validation (e.g., RNA-seq) of the identified variants. Additionally, the small cohort size ($n = 8$) may reduce statistical power for genotype-phenotype correlations. Although HuH-7/HepG2 cells recapitulate hepatic MRP2 function, their transformed nature and lack of polarized architecture may not fully mirror in vivo hepatobiliary physiology. The use of overexpression systems in HEK293T could also introduce artifactual effects. The clinical relevance of our findings may be influenced by population-specific genetic backgrounds, and the absence of longitudinal clinical data limits assessment of phenotypic progression. Functional assays were performed under controlled conditions that may not capture the complexity of metabolic interactions in patients. Future studies incorporating patient-derived iPSCs, larger multi-ethnic cohorts, and longitudinal monitoring will help address these limitations.

In summary, we describe a splice-site variant (c.2439 + 5G > A) in *ABCC2* gene, which induces aberrant splicing within intron 18. To our knowledge, this is the first study to elucidate its pathogenic mechanism. Both in silico predictions and minigene assays consistently demonstrated that this variant causes complete exon 18 skipping (r.2272_2439del), resulting in an in-frame deletion of 56 amino acids (p.Gly758_Lys813del) in the MRP2 protein. Functional analysis revealed that the c.2439 + 5G > A variant significantly reduced MRP2 expression and impaired its organic anion transport activity, supporting the classification of c.2439 + 5G > A as a pathogenic variant. Our findings highlight the critical importance of *ABCC2* genetic testing in patients with unexplained conjugated hyperbilirubinemia, enabling accurate diagnosis and clinical management of DJS.

Abbreviations

DJS	Dubin-johnson syndrome
WES	Whole exome sequencing
WB	Western blot
IF	Indirect immunofluorescence
MRP2	Multi-drug resistance protein 2
MSDs	Membrane-spanning domains
NBDs	Nucleotide-binding domains
ABC	ATP-binding cassette
UTRs	Untranslated regions
gDNA	Genomic DNA
WT	Wild-type
TB	Total bilirubin
DB	Direct bilirubin
AFP	Alpha-fetoprotein
ALT	Alanine transaminase

AST	Glutamic oxaloacetic transaminase
MCB	Monochlorobimane
GSH	Glutathione

Supplementary Information

The online version contains supplementary material available at https://doi.org/10.1186/s12920-025-02187-4.

Supplementary Material 1

Supplementary Material 2

Acknowledgements
We are grateful to the patient and his family for their understanding and cooperation, and to express gratitude to Berry Genomics Co., for the technical support received.

Author contributions
RYS and TMZ drafted the article. YMC and DW conceived the study and revised the manuscript. YZL collected clinical data and investigated the data. TTJ and CJG analyzed the data. RTW performed the bioinformatic analysis. RYS, CJG, YW, FZX and SKF performed the experiments. All authors contributed to revising the manuscript and read through and approved the submitted version.

Funding
This work was supported by the National Natural Science Foundation of China (82171701), and the Medical Science and Technology Project of Zhejiang Province (2022YK839).

Data availability
The datasets generated and/or analyzed during the current study are available from the corresponding author upon reasonable request. The novel variant revealed in the study were submitted to ClinVar database (https://www.ncbi.nlm.nih.gov/clinvar/) under Accession Numbers SCV005687770.

Declarations

Ethics approval and consent to participate
The study was conducted by the Declaration of Helsinki and approved by the ethics committee of The First Affiliated Hospital of Wenzhou Medical University (No. YS2024-268). Informed consent to participate was obtained from all of the participants and parents of the minor participant in the study.

Consent for publication
Not applicable.

Competing interests
The authors declare no competing interests.

Author details
[1]Department of Pulmonary and Critical Care Medicine, People's Hospital of Jingning She Autonomous County, Lishui 323000, Zhejiang, P. R. China
[2]Department of Surgery, The Second Affiliated Hospital, Yuying Children's Hospital of Wenzhou Medical University, No.109 Xueyuan West Road, Wenzhou 325000, Zhejiang, P. R. China
[3]Department of Pediatrics, The First Affiliated Hospital of Wenzhou Medical University, No.2 Fuxue Road, Wenzhou 325000, Zhejiang, P. R. China
[4]Department of Pediatrics, Taizhou Hospital of Zhejiang Province Affiliated to Wenzhou Medical University, Linhai 317000, Zhejiang, P. R. China
[5]Department of Pediatrics, Lishui People's Hospital, Lishui 323000, Zhejiang, P. R. China
[6]Department of Orthopedics, People's Hospital of Jingning She Autonomous County, Lishui 323000, Zhejiang, P. R. China

Received: 21 January 2025 / Accepted: 9 July 2025
Published online: 18 July 2025

References

1. Mao YX, et al. Transport mechanism of human bilirubin transporter ABCC2 tuned by the inter-module regulatory domain. Nat Commun. 2024;15(1):1061.
2. Strassburg CP. Hyperbilirubinemia syndromes (Gilbert-Meulengracht, Crigler-Najjar, Dubin-Johnson, and rotor syndrome). Best Pract Res Clin Gastroenterol. 2010;24(5):555–71.
3. Memon N, et al. Inherited disorders of bilirubin clearance. Pediatr Res. 2016;79(3):378–86.
4. Dubin IN, Johnson FB. Chronic idiopathic jaundice with unidentified pigment in liver cells; a new clinicopathologic entity with a report of 12 cases. Med (Baltim). 1954;33(3):155–97.
5. Paulusma CC, et al. A mutation in the human canalicular multispecific organic anion transporter gene causes the Dubin-Johnson syndrome. Hepatology. 1997;25(6):1539–42.
6. Wada M, et al. Mutations in the canilicular multispecific organic anion transporter (cMOAT) gene, a novel ABC transporter, in patients with hyperbilirubinemia II/Dubin-Johnson syndrome. Hum Mol Genet. 1998;7(2):203–7.
7. Corpechot C, et al. Genetic contribution of ABCC2 to Dubin-Johnson syndrome and inherited cholestatic disorders. Liver Int. 2020;40(1):163–74.
8. Wang NL, et al. A specially designed Multi-Gene panel facilitates genetic diagnosis in children with intrahepatic cholestasis: simultaneous test of known large insertions/deletions. PLoS ONE. 2016;11(10):e0164058.
9. Li M, Kong XY, Wang SM. Effects of splicing-regulatory polymorphisms in ABCC2, ABCG2, and ABCB1 on methotrexate exposure in Chinese children with acute lymphoblastic leukemia. Cancer Chemother Pharmacol. 2023;91(1):77–87.
10. Brandi G, et al. Wilson disease, ABCC2 c.3972C > T polymorphism and primary liver cancers: suggestions from a Familial cluster. BMC Med Genet. 2020;21(1):225.
11. Fardel O, et al. Physiological, Pharmacological and clinical features of the multidrug resistance protein 2. Biomed Pharmacother. 2005;59(3):104–14.
12. Kimura A, et al. Rotor syndrome: glucuronidated bile acidemia from defective reuptake by hepatocytes. Hepatol Commun. 2021;5(4):629–33.
13. Wu L, et al. A recurrent ABCC2 p.G693R mutation resulting in loss of function of MRP2 and hyperbilirubinemia in Dubin-Johnson syndrome in China. Orphanet J Rare Dis. 2020;15(1):74.
14. Li D, et al. Neurodegenerative diseases: a hotbed for splicing defects and the potential therapies. Transl Neurodegener. 2021;10(1):16.
15. Hinkle ER, et al. RNA processing in skeletal muscle biology and disease. Transcription. 2019;10(1):1–20.
16. Montes M, et al. RNA splicing and disease: animal models to therapies. Trends Genet. 2019;35(1):68–87.
17. Scotti MM, Swanson MS. RNA mis-splicing in disease. Nat Rev Genet. 2016;17(1):19–32.
18. Lee JH, et al. Neonatal Dubin-Johnson syndrome: long-term follow-up and MRP2 mutations study. Pediatr Res. 2006;59(4 Pt 1):584–9.
19. Fu H, et al. Neonatal Dubin-Johnson syndrome: biochemical parameters, characteristics, and genetic variants study. Pediatr Res. 2022;91(6):1571–8.
20. Richards S, et al. Standards and guidelines for the interpretation of sequence variants: a joint consensus recommendation of the American college of medical genetics and genomics and the association for molecular pathology. Genet Med. 2015;17(5):405–24.
21. Park SW, et al. Hepatobiliary and pancreatic: A black liver of Dubin-Johnson syndrome. J Gastroenterol Hepatol. 2018;33(3):562.
22. Kartenbeck J, et al. Absence of the canalicular isoform of the MRP gene-encoded conjugate export pump from the hepatocytes in Dubin-Johnson syndrome. Hepatology. 1996;23(5):1061–6.
23. Trauner M, Boyer JL. Bile salt transporters: molecular characterization, function, and regulation. Physiol Rev. 2003;83(2):633–71.
24. Mottino AD, et al. Altered localization and activity of canalicular Mrp2 in estradiol-17beta-D-glucuronide-induced cholestasis. Hepatology. 2002;35(6):1409–19.
25. Wang JQ, et al. Multidrug resistance proteins (MRPs): structure, function and the overcoming of cancer multidrug resistance. Drug Resist Updat. 2021;54:100743.
26. Togawa T, et al. Clinical, pathologic, and genetic features of neonatal Dubin-Johnson syndrome: A multicenter study in Japan. J Pediatr. 2018;196:161–e1671.
27. Kimura A, et al. Neonatal Dubin-Johnson syndrome with severe cholestasis: effective phenobarbital therapy. Acta Paediatr Scand. 1991;80(3):381–5.

28. Regev RH, et al. Treatment of severe cholestasis in neonatal Dubin-Johnson syndrome with ursodeoxycholic acid. J Perinat Med. 2002;30(2):185–7.
29. Bremmelgaard A, Sjövall J. Hydroxylation of cholic, chenodeoxycholic, and deoxycholic acids in patients with intrahepatic cholestasis. J Lipid Res. 1980;21(8):1072–81.
30. Wagner M, Zollner G, Trauner M. New molecular insights into the mechanisms of cholestasis. J Hepatol. 2009;51(3):565–80.
31. Okada H, et al. Neonatal Dubin-Johnson syndrome: novel compound heterozygous mutation in the ABCC2 gene. Pediatr Int. 2014;56(5):e62–4.
32. Hashimoto K, et al. Trafficking and functional defects by mutations of the ATP-binding domains in MRP2 in patients with Dubin-Johnson syndrome. Hepatology. 2002;36(5):1236–45.
33. Meng LL, et al. [Clinical features and ABCC2 genotypic analysis of an infant with Dubin-Johnson syndrome]. Zhongguo Dang Dai Er Ke Za Zhi. 2019;21(1):64–70.
34. Chen HL, et al. Panel-Based Next-Generation sequencing for the diagnosis of cholestatic genetic liver diseases: clinical utility and challenges. J Pediatr. 2019;205:153–e1596.

Publisher's note

Springer Nature remains neutral with regard to jurisdictional claims in published maps and institutional affiliations.